Fachtagung "Experimentelle Strömungsmechanik"
3. – 5. September 2019, Erlangen

Aerodynamic loads on a cyclist while overtaking by a vehicle

Aerodynamische Kraftwirkung auf einen Fahrradfahrer beim Überholvorgang durch ein Fahrzeug

Christof Gromke[1,*], Bodo Ruck[1]
[1]Karlsruhe Institute of Technology KIT, Institute for Hydromechanics, Laboratory of Building- and Environmental Aerodynamics, Karlsruhe, Germany
[*]gromke@kit.edu

Key words: vehicle-induced load, cyclist safety, flip over load, overtaking maneuver
Schlagworte: Fahrzeug-induzierte Kraft, Fahrradsicherheit, Lastumschlag, Überholmanöver

Abstract

Road vehicle-induced aerodynamic loads on a cyclist during overtaking maneuvers were acquired in full-scale measurements. In an experiment series with a passenger car and an adult dummy on a city bike, time series of pressure and suction loads were measured. Overtaking maneuvers with various passing distances (0.5 - 2.0 m) and vehicle speeds (40 - 100 km/h) were carried out. As a highly interesting and relevant element for cyclist safety, a rapid flip over from pressure to suction load acting on the cyclist during the overtaking maneuver was measured. The flip over was quantified in terms of the extent of the load change (peak-to-peak value) and its duration. Based on that, a new parameter, the ratio of flip over load to flip over duration (flip over load rate) was introduced. Correlations between the flip over load rate and the passing distance, and vehicle speed were found and functional relationships were established.

Introduction

The overtaking of cyclists by road vehicles is a typical process in everyday traffic situations in cities as well as in interurban areas. During an overtaking, the cyclist experiences a transient aerodynamic load consisting of a sequence of pressure and suction load phases with major components in the direction of travel and lateral to it. The strength and duration of the pressure and suction load phases are basically determined by the vehicle speed and size (type), passing distance, the cyclist's size and posture, and the cycle type and equipment.
For an ordinary overtaking maneuver, the following 5 main phases and fundamental characteristics in the time series of the vehicle-induced pressure and suction load acting lateral to the driving direction can be identified, see also Fig. 2:

- p1: A phase with an increasing pressure load which acts to push the cyclist away from the vehicle while it is approaching. During that phase, the pressure load is progressively increasing in time.

GALA e.V., Karlsruhe, Germany, ISBN 978-3-9816764-6-4

- p2: A phase with a relatively rapid flip over from pressure to suction load. The flip over occurs when the vehicle front is next to the front half of the cyclist.
- p3: A phase with a predominant suction load which acts to pull the cyclist towards the overtaking vehicle. In this phase, the load fluctuates and may, occasionally, for short time intervals, act as a pressure load on the cyclist.
- p4: A phase with a second (reverse) flip over from suction to pressure with a magnitude smaller than that of the first flip over from pressure to suction observed in phase 2.
- p5: In the final phase, when the vehicle has overtaken the cyclist, the load declines to zero superimposed by decaying oscillation-like fluctuations of small amplitude induced by the vehicle wake.

From a cyclist and traffic safety point of view, the second phase with the rapid flip over from pressure to suction load is the most interesting and relevant one. The rapid flip over can possibly induce an unexpected but noticeable disturbance in driving and additionally trigger a reflexive and uncontrolled compensatory maneuver by the cyclist. Conceivably, the cyclist may tumble or collide with the overtaking vehicle or roadside objects. Such an uncontrolled maneuver may, in addition to the cyclist safety, also impair the safety of other traffic participants.
Despite its importance and increasing topicality, the subject has not been a matter of research so far and knowledge about road vehicle-induced loads acting on cyclists while overtaking is completely lacking. A survey on vehicle-induced aerodynamic loads on humans shows that past studies have rather addressed train-induced pressure and suction loads and their relevance for the safety of persons or stability of objects at platforms (Gerhardt and Krüger 1998, Sanz-Andres and Santiago-Prowald 2002, Sanz-Andres et al. 2004, Sterling et al. 2008, Federal Railroad Administration 2009, Baker et al. 2014, Zhou et al. 2014, Khayrullina et al. 2015). These studies were stimulated because platforms are often in an environment where the space is confined and, hence, higher aerodynamic loads may be expected than in unconfined spaces. Studies on road vehicle-induced aerodynamic loads are limited to pressure and suction loads on roadside pedestrian barriers, traffic panels, flat plates and walls (Cali and Covert 2000, Quinn et al. 2001, Sanz-Andres et al. 2003, Sanz-Andres et al. 2004, Lichtneger and Ruck 2015, Lichtneger and Ruck 2018). However, studies on road vehicle-induced aerodynamic loads on cyclists are lacking so far. In the focus of the present study is the quantification of the lateral pressure and suction loads a cyclist experiences when overtaken by a passenger car.

Material and Methods

Lateral Pressure and suction loads exerted on a cyclist by an overtaking passenger car were measured in a field measurement campaign. A bike-dummy assembly, consisting of a life-size dummy of an adult person wearing a jumpsuit sitting on a city bike (aka touring bike), was attached to a rack by means of 4 truss members (Fig. 1). The rack and the dummy-bike assembly were placed at the edge of a road of a 700 m long straight street section.
In an experiment series, overtaking maneuvers with different vehicle speeds passing the bike-dummy assembly at different distances were performed. The passing distance is the spacing between the car envelope (excluding the protruding side mirrors) and the central vertical plane of the bike-dummy assembly defined by the bicycle frame. Combinations of overtaking maneuvers of nominal (= targeted) vehicle speeds V_{veh} of 40, 60, 80 and 100 km/h (corresponding to 11.1, 16.7, 22.2 and 27.8 m/s) and passing distances d_{pass} of 0.5,

GALA e.V., Karlsruhe, Germany, ISBN 978-3-9816764-6-4

1.0, 1.5 and 2.0 m were realized. Every speed-distance combination was repeated 5 times and summarized in an ensemble-average.
A station wagon (type Audi A4 Avant) was employed as a representative for the class of passenger cars. Forces were measured with 4 uniaxial S-beam load cells (type Althen SL25) in combination with tuned measurement amplifiers (type Althen SG-KP-12E-B10). Runs were recorded during calm wind conditions with ambient wind speeds below 1.4 m/s at 1.7 m above ground in order to avoid too strong biasing of the force sensor signals. The actual passing distance was acquired by a distance sensor (type ifm O1D100). The actual passing speed was controlled by the car's cruise control and additionally derived from signal outputs from two photoelectric sensors.

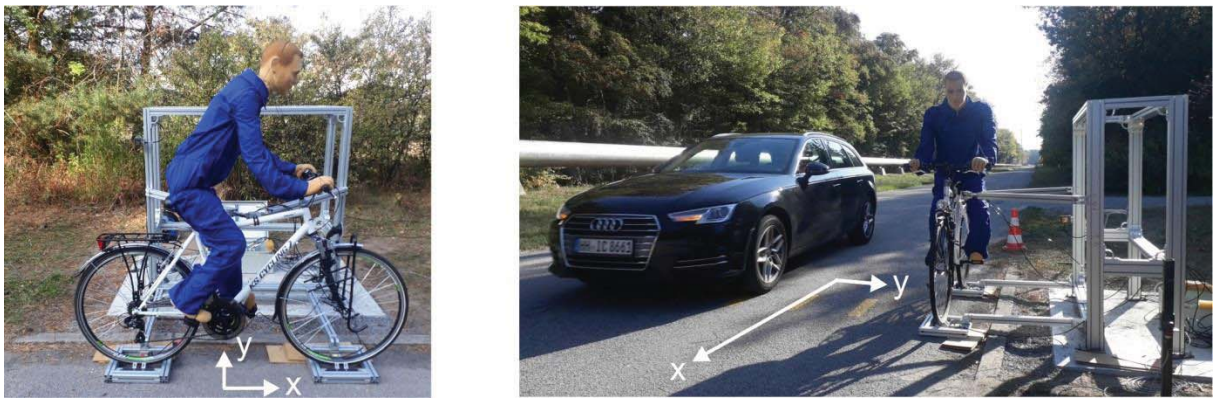

Fig 1: Dummy-bike assembly mounted on rack (left), snapshot of passenger car during overtaking maneuver.

Results and Discussion

Fig. 2 shows as an example the ensemble-averaged time series of the resultant lateral vehicle-induced load $F_{res,y}$ acting on the adult dummy on the city bike (dummy-bike assembly). The data were obtained for overtaking maneuvers with the passenger car at nominal vehicle speed and passing distance of V_{veh} = 80 km/h and d_{pass} = 1.0 m, respectively (actual values of the individual runs: 78.5 km/h ≤ V_{veh} ≤ 78.7 km/h and 1.09 m ≤ d_{pass} ≤ 1.17 m). In the diagram, the zero-timestamp coincides with the passing of the vehicle front at the first photoelectric sensor which is positioned 0.95 m in front of the backmost part of the rear wheel. The solid line shows the unfiltered load data and the dash-dotted line the load data filtered by a 6^{th} order zero-phase delay low-pass Butterworth filter with cutoff frequency f_{co} = 12 Hz. The cutoff frequency was chosen such that the basic signal characteristics were retained but the higher frequency trembling-like fluctuations which are attributed to an excitation of the dummy-bike assembly by ground vibrations due to the passing vehicle were removed.
As an indication for the position of the vehicle relative to the bicycle, the rectangular box spans the period starting when the foremost vehicle part passes the backmost part of the rear wheel (left edge) and ending when the backmost vehicle part passes the foremost part of the front wheel (right edge). The horizontal bar indicates the passing period with reference to the bottom bracket of the bicycle which is approximately the horizontal centroid of area (x_c) of the dummy-bike assembly.
The five phases p1 to p5 as described in the Introduction section are indicated in Fig. 2:

- p1: phase with increasing pressure load,
- p2: flip over phase (rapid load change from pressure to suction),
- p3: suction load phase,

GALA e.V., Karlsruhe, Germany, ISBN 978-3-9816764-6-4

- p4: reverse flip over phase (relatively rapid load change from suction to pressure),
- p5: phase with decaying oscillation-like fluctuations.

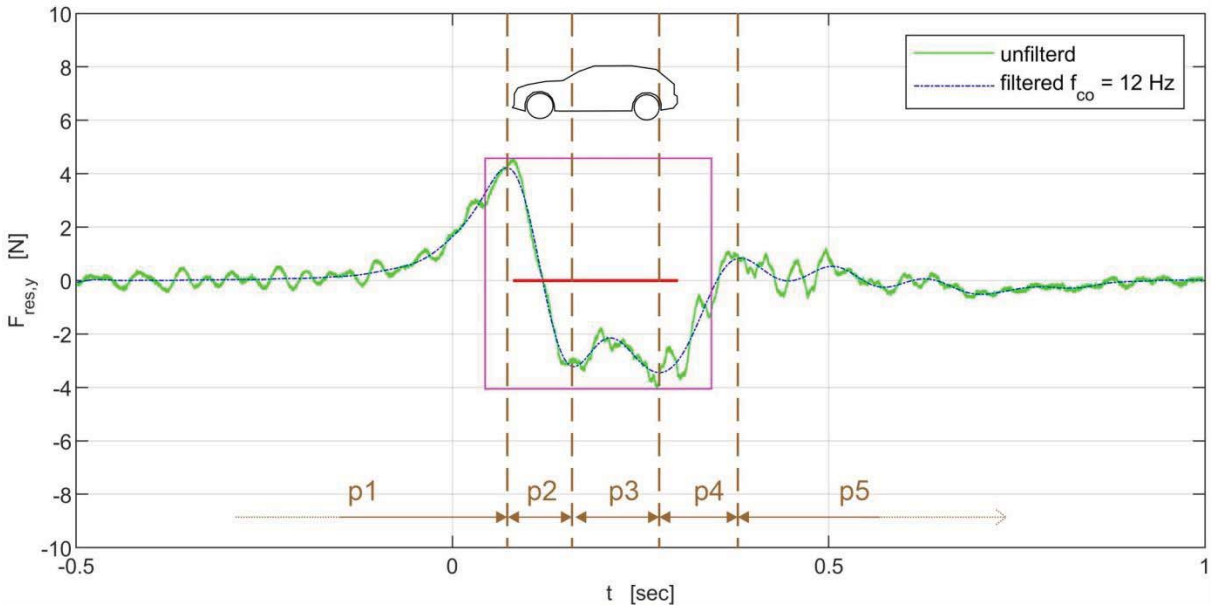

Fig 2: Ensemble-averaged time series of resultant lateral vehicle-induced load on dummy-bike assembly (adult dummy on city bike) obtained from 5 repeated runs of a passenger car (station wagon) with nominal speed and passing distance V_{veh} = 80 km/h and d_{pass} = 1.0 m.

For the current case, the load cells started to noticeably register the approaching vehicle (onset of phase p1) approximately 0.2 s before the foremost part of the passenger car passed the backmost part of the rear wheel (left edge of the rectangular box). In this phase, the pressure load progressively increased until it reached a maximum shortly before the foremost vehicle part passed the bottom bracket. The following flip over phase extended over 0.08 s in which the cyclist was subjected to a jump from a pressure load of 4.2 N to a suction load of 3.2 N (peak-to-peak load $\Delta F_{res,y}$ = 7.5 N). Here, the flip over is initiated closely after the front part of the vehicle passes the bottom bracket of the cycle. In phase 3, the suction load phase, the vehicle-induced lateral load stayed on a relatively constant level of around 3 N lasting for 0.12 s. The end of the suction load phase closely coincided with the passing of the backmost vehicle part at the bottom bracket. In the following reverse flip over phase with duration of 0.11 s, the load direction changed and, at its end, the cyclist was exposed to a pressure load of 0.9 N. During that phase, the passenger car has completely passed the dummy-bike assembly. In the final phase, the load faded out in an oscillatory manner. The load oscillations are attributed to regularly alternating flow structures in the vehicle's wake.
Since from a cyclist and traffic safety point of view, the rapid load jump from pressure to suction load is highly relevant, the following analysis focuses on the analysis of the flip over characteristics of phase p2. Fig. 3 displays the ensemble-averaged flip over loads ΔF obtained from overtaking maneuvers of the adult dummy on the city bike. The left panel shows the flip over load versus the vehicle speed for sets of constant nominal passing distance. The right panel shows the flip over load versus the passing distance for sets of constant nominal vehicle speed. Overall, the flip over loads are in a range between 0.5 N < ΔF < 31.1 N. For comparison, in full-scale studies performed by the Federal Railroad Administration (2009) with high-speed trains passing a circular cylindrical instrumented dummy (CID) standing at a lateral distance of 1.20 m away from the side of the train, flip over loads induced by the train head of ΔF = 69 N for an Acela Express train at 239 km/h, of ΔF = 125 N for an Amfleet train

GALA e.V., Karlsruhe, Germany, ISBN 978-3-9816764-6-4

with AEM-7 locomotive at 184 km/h, and of ΔF = 62 N for an Amfleet train with HHP-8 locomotive at 201 km/h were measured. The circular cylindrical instrumented dummy (CID) is a representation of the generic geometry of the human body. It consists of a cylinder with diameter of 0.39 m and axial length of 0.92 m supported on a post with its bottom side being approximately 0.65 m above ground.

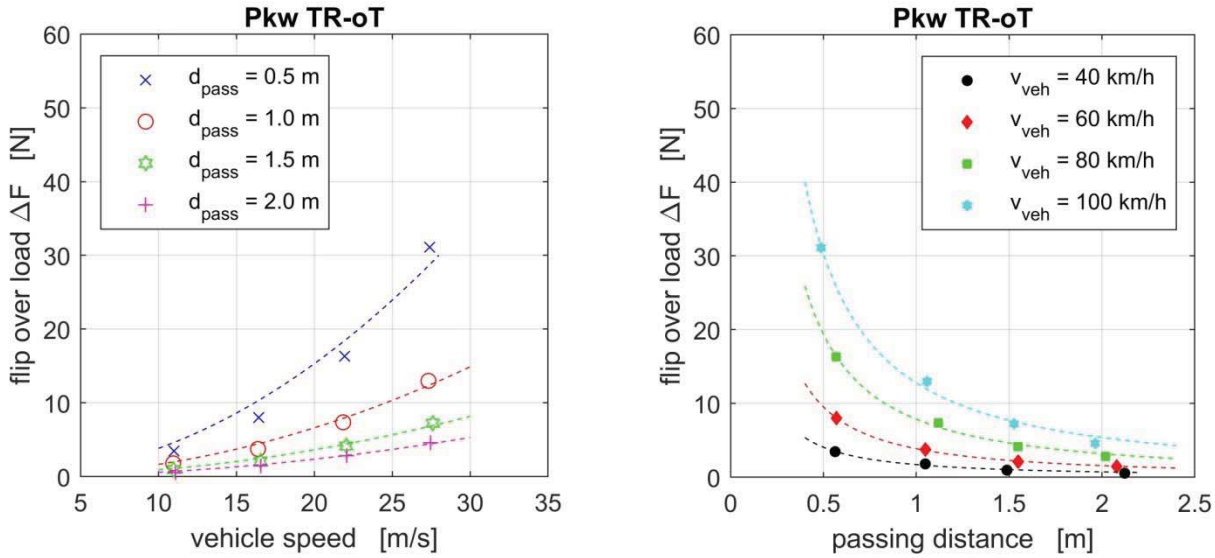

Fig 3: Flip over loads ΔF (ensemble-averaged) obtained from overtaking maneuvers of the adult dummy on the city bike.

From the left panel, it can be seen that – as expected – the flip over load increases with increasing vehicle speed and is larger for smaller passing distances. A fit of the data by a power function of type $\Delta F = c_1 \cdot (V_{veh})^2$ yields for the pre-factor values of c_1 [kg/m] = {0.038, 0.017, 0.009, 0.006} for passing distances d_{pass} [m] = {0.5, 1.0, 1.5, 2.0}, respectively, with corresponding coefficients of determination R^2 = {0.962, 0.984, 0.986, 0.991}. The fitted curves are indicated as dashed lines in the left panel of Fig. 3. The exponent in the power function was set a priori to 2 based on the well established quadratic relation between fluid dynamical load and fluid velocity (= vehicle speed) for turbulent flows. However, the coefficient of determination decreases with decreasing passing distance, indicating a deviation of the actual value of the exponent from 2 – in particular for smaller passing distances. The deterioration of the fit for smaller passing distances is also visually apparent in the diagram. It is hypothesized that the deviation can be attributed to the transient and spatially inhomogeneous load impact induced by the passing vehicle. In addition to its unsteadiness in time, the propagation of the vehicle accompanying flow field results in an inhomogeneous load impact of the various parts of the dummy-bike assembly in driving direction (e.g. rear wheel, dummy, front wheel). A larger passing distance, however, allows for an equalization of differences in the flow field due to turbulent exchange of momentum and promotes an homogenization of the flow field while propagating perpendicular to the driving direction. The impacting vehicle-induced wind load on the dummy-bike assembly is more uniform for larger passing distances and, hence, conforms more closely to the flow condition under which the quadratic relation between wind load and wind velocity holds.
From the right panel, it can be seen that – also as expected – the flip over load decreases with increasing passing distance and is larger for higher vehicle speeds. A fit of the data by a power function of type $\Delta F = c_2 \cdot (d_{pass})^{\alpha}$ yields for the pre-factor values of c_2 = {1.7, 3.9, 7.9, 12.8} and for the exponent α = {-1.25, -1.30, -1.30, -1.24} for vehicle speeds

GALA e.V., Karlsruhe, Germany, ISBN 978-3-9816764-6-4

V_{veh} [km/h] = {40, 60, 80, 100}, respectively. The corresponding coefficients of determination are R^2 = {0.988, 0.999, 0.995, 0.995} and the fitted curves are indicated as dashed lines in the right panel of Fig. 3. The exponents assume values around -1.3 and thus reflect the expected reduction of the vehicle-induced load with distance for the given geometric boundary conditions with $-2 < \alpha < -1$. Since the ground inhibits a propagation at the lower surface, the vehicle-induced load can only spread upwards and to the left and right in the horizontal plane. Instead of a 2-dimensional spreading of the load in a plane perpendicular to its propagation path, where ideally $\alpha = -2$, the spreading is limited to 1.5 dimensions and the reduction of the vehicle-induced load with distance occurs slower, reflected by exponents α laying between -2 and -1.
The ensemble-averaged flip over durations Δt, i.e. the durations of phase p2, are shown in Fig. 4. The left panel shows the flip over durations versus the vehicle speed for sets of constant nominal passing distance and the right panel shows the flip over duration versus the passing distance for sets of constant nominal vehicle speed. Overall, the flip over durations are between $0.07\ s < \Delta t < 0.24\ s$.

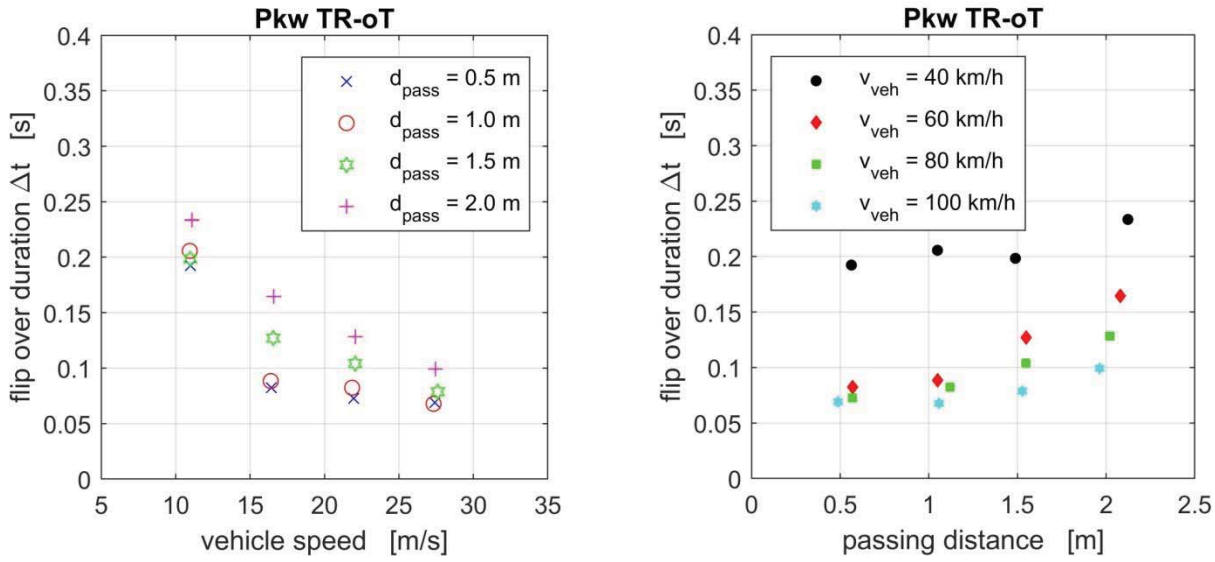

Fig 4: Flip over durations Δt (ensemble-averaged) obtained from overtaking maneuvers of the adult dummy on the city bike.

From the left panel, it can be seen that the flip over duration decreases with increasing vehicle speed and is generally longer for larger passing distances. Excluding the slowest vehicle speed (11.1 m/s = 40 km/h), the decreases display a linear characteristic for all sets of constant passing distance. For sets of constant vehicle speeds (right panel Fig. 4), the flip over duration shows the overall tendency to increase with increasing passing distance. The flip over durations for the slowest vehicle speed (V_{veh} = 40 km/h) are markedly longer than for the other speeds, in particular for the smaller passing distances, and the tendency of increasing flip over duration with increasing passing distance is less pronounced.
For an assessment of the cyclist and traffic safety, not only the strength of the flip over load ΔF is of interest, but also the duration Δt of the flip over. Evidently, the reaction of a cyclist to a change in load by a compensatory maneuver depends on the rapidness of the process. In particular the cyclist's control over the steering motion during the compensatory maneuver is significantly affected by the duration of the flip over load. A slow change in load can be responded to by the cyclist by relatively smooth and small increments in steering motion, hence, by a controlled reaction. A rapid change in load, however, is prone to be responded to

GALA e.V., Karlsruhe, Germany, ISBN 978-3-9816764-6-4

by relatively abrupt and large increments in steering motion and is more likely to trigger an overreaction leading to an uncontrolled driving maneuver. Therefore, the ratio ΔF/Δt of flip over load to flip over duration (flip over load rate) is introduced. Fig. 5 presents ensemble-averaged ratios ΔF/Δt obtained from the overtaking maneuvers. The left panel of Fig. 5 depicts ratios ΔF/Δt versus the vehicle speed for sets of constant passing distance and the right panel shows ratios ΔF/Δt versus the passing distance for sets of constant vehicle speed.

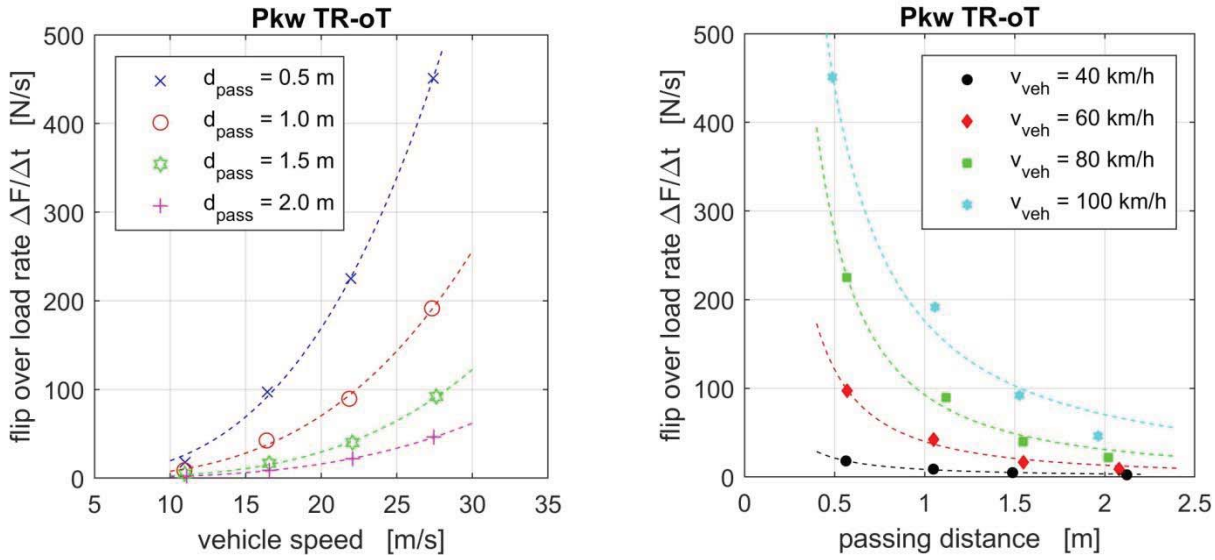

Fig 5: Ratios of flip over load and flip over duration ΔF/Δt (ensemble-averaged) obtained from overtaking maneuvers of the adult dummy on the city bike.

The regularities and clear tendencies observable for the sets of constant passing distance (Fig. 5, left panel) and constant vehicle speed (Fig. 5, right panel) imply that the ratio of flip over load to duration is a meaningful and stressable parameter. The dashed lines in the left and right panel of Fig. 5 are curve fits obtained on the basis of power functions of type $\Delta F/\Delta t = c_3 \cdot (V_{veh})^{\beta}$ and $\Delta F/\Delta t = c_4 \cdot (d_{pass})^{\gamma}$, respectively. The low scatter among the exponents of the power functions with $3.1 < \beta < 3.5$ and $-1.6 < \gamma < -1.3$ as well as the high coefficients of determination R^2 (> 0.984 always) further substantiate the appropriateness of the ratio of flip over load to duration as a meaningful and stressable parameter.

Summary and Conclusions

Flip over characteristics of rapid load changes from pressure to suction acquired in a full-scale measurement series with a passenger car (station wagon) overtaking an adult dummy sitting on a city bike were analyzed and evaluated. The main parameters characterizing a flip over are the load difference ΔF induced by the rapid change from pressure to suction, its duration Δt, and the ratio of flip over load to flip over duration ΔF/Δt (flip over load rate). In the present study, flip over loads in the range between 0.5 N < ΔF < 31.1 N and flip over durations between 0.07 s < Δt < 0.24 s were obtained. The flip over loads showed an increase with increasing vehicle speed and decreasing passing distance. Power functions with exponents of 2 and ≈ -1.3 were found appropriate for a quantitative description of the relation between flip over load and vehicle speed or passing distance, respectively. The flip over durations showed a decrease with increasing vehicle speed and an overall increase with increasing passing distance. For the flip over load rate ΔF/Δt, values in the range between 2.3 and

GALA e.V., Karlsruhe, Germany, ISBN 978-3-9816764-6-4

451.1 N/s were determined in the present study. The flip over load rate was found to increase with vehicle speed and decrease with passing distance. Employing power functions, relationships between the flip over load rate and vehicle speed, with exponents close to 3.3, and between flip over load rate and passing distance, with exponents close to -1.4, could be established. It is concluded that because of the low scatter among the exponents of the respective power functions and the high degree of correlations, the flip over load rate is a meaningful and stressable parameter for the characterization of the flip over process.

Acknowledgements

The authors gratefully acknowledge the financial support of the Deutsche Forschungsgemeinschaft DFG (German Research Foundation) under grant Ru 345/32-3.

References

Baker, C.J., Jordan, S., Gilbert, T., Quinn, A.D., Sterling, M., Johnson, T., Lane, J., 2014: “Transient aerodynamic pressures and forces on trackside and overhead structures due to passing trains, Part 1 - Part 2”, Proceedings of the Institution of Mechanical Engineers, Part F: Journal of Rail and Rapid Transit, Vol. 228, pp. 37-70

Cali, P.M., Covert, E.E., 2000: “Experimental measurements of the loads induced on an overhead highway sign structure by vehicle-induced gusts”, Journal of Wind Engineering and Industrial Aerodynamics, Vol. 84, pp. 87-100

Federal Railroad Administration, 2009: "The aerodynamic effects of passing trains on surrounding objects and people", U.S. Department of Transportation, Office of Research and Development, Final Report, pp. 257

Gerhardt, H.J., Krüger, O., 1998: “Wind and train driven air movements in train stations”, Journal of Wind Engineering and Industrial Aerodynamics, Vol. 74-76, pp. 589-597

Khayrullina, A., Blocken, B., Janssen, W., Straathof, J., 2015: “CFD simulation of train aerodynamics - Train-induced wind conditions at an underground railroad passenger platform”, Journal of Wind Engineering and Industrial Aerodynamics, Vol. 139, pp. 100-110

Lichtneger, P., Ruck, B., 2015: “Full scale experiments on vehicle induced transient loads on roadside plates”, Journal of Wind Engineering and Industrial Aerodynamics, Vol. 136, pp. 73-81

Lichtneger, P., Ruck, B., 2018: “Full scale experiments on vehicle induced transient pressure loads on roadside walls”, Journal of Wind Engineering and Industrial Aerodynamics, Vol. 174, pp. 451-457

Quinn, A.D., Baker, C.J., Wright, N.G., 2001: “Wind and vehicle induced forces on flat plates - Part 2: vehicle induced force”, Journal of Wind Engineering and Industrial Aerodynamics, Vol. 89, pp. 831-847

Sanz-Andres, A., Santiago-Prowald, J., 2002: “Train-induced pressure on pedestrians”, Journal of Wind Engineering and Industrial Aerodynamics, Vol. 90, pp. 1007-1015

Sanz-Andres, A., Santiago-Prowald, J., Baker, C.J., Quinn A.D., 2003: “Vehicle-induced loads on traffic sign panels”, Journal of Wind Engineering and Industrial Aerodynamics, Vol. 91, pp. 925-942

Sanz-Andres, A., Laveron, A., Baker, C.J., Quinn, A., 2004: “Vehicle induced loads on pedestrian barriers”, Journal of Wind Engineering and Industrial Aerodynamics, Vol. 92, pp. 413-426

Sanz-Andres, A., Laveron, A., Cuerva, A., Baker, C.J., 2004: “Vehicle-induced forces on pedestrians”, Journal of Wind Engineering and Industrial Aerodynamics, Vol. 92, pp. 185-198

Sterling, M., Baker, C.J., Jordan, S.C., Johnson, T., 2008: “A study of the slipstreams of high-speed passenger trains and freight trains”, Proceedings of the Institution of Mechanical Engineers, Part F: Journal of Rail and Rapid Transit, Vol. 222, pp. 177-193

Zhou, D., Tian, H., Zhang, J., Yang, M., 2014: “Pressure transients induced by a high-speed train passing through a station”, Journal of Wind Engineering and Industrial Aerodynamics, Vol. 135 pp. 1-9

GALA e.V., Karlsruhe, Germany, ISBN 978-3-9816764-6-4